ELSEVIER

Precambrian Research 104 (2104) 187–206

Precambrian Research

www.elsevier.com/locate/precamres

2.8–3.0 Ga plutonism and deformation in the SE Amazonian craton: the Archaean granitoids of Marajoara (Carajás Mineral Province, Brazil)

Fernando Althoff [a,b], Pierre Barbey [b,*], Anne-Marie Boullier [c]

[a] *UNISINOS, CP 275, 93001-970 São Leopoldo RS, Brazil*
[b] *CRPG-CNRS, B.P. 20, F-54501 Vandoeuvre-Nancy Cedex, France*
[c] *LGIT-CNRS, B.P. 53, F-38041 Grenoble Cedex 9, France*

Received 8 June 1999; accepted 14 July 2000

Abstract

The granitoids of Marajoara in the Rio Maria terrain (Carajás Mineral Province, Brazil) consist of: (i) a broad unit of 2.96 Ga syntectonic tonalites (Arco Verde Tonalites) displaying a trondhjemitic differentiation trend; (ii) 2.93 Ga syntectonic monzogranites (Guarantã); and (iii) 2.87 Ga post-tectonic monzogranites (Mata Surrão) and granodiorites (Rio Maria), displaying a calc-alkaline differentiation trend. Deformation of the Arco Verde tonalites is heterogeneous with low strain domains (well preserved magmatic banding and textures) and orthogneissic domains displaying an E–W trending mainly subvertical foliation, associated with horizontal lineations, upright folds and subvertical shear zones. Microstructures and phase assemblages suggest that deformation occurred within a large temperature range (i.e. during magma emplacement and cooling), from high-T conditions (synmagmatic shear zones and subsolidus ductile deformation with intense quartz and feldspar recrystallization; Pl + Qtz + Hbl + Bt assemblages) to medium- and low-T conditions (ductile to brittle deformation with weakly recrystallized quartz and undulose extinction in feldspars; Qtz + Pl + Bt + Mu or Chl + Ep + Ab + Qtz assemblages). These data, finite strain analysis and structures reported from the surrounding greenstone belts suggest that deformation did not result from a post-emplacement prograde tectono-metamorphic event as considered previously, but that the Marajoara granitoids are synkinernatic intrusions which were deformed together with the supracrustal rocks during a regional NS horizontal shortening. Although the Rio Maria terrain presents similarities with Archaean domains controlled by diapiric processes (lithologies dominated by thick greenstone sequences and TTG plutons, and forming a dome-and-keel structure), its structural evolution is controlled dominantly by a transpressional event which shaped the granite–greenstone terrains. The Rio Maria area, probably as many Archaean 'grey gneisses' domains, represents an intermediate case between terrains controlled by Raleigh–Taylor instabilities in a thermally softened crust with insignificant external forces related to plate convergence (e.g. east Pilbara craton) and those controlled by thrust tectonics related to convergence of rigid plates (e.g. Superior Province). The closest analog to the Rio Maria terrain seems to be the Chilimanzi area in the Zimbabwe craton.

Keywords: South America; Amazonian craton; Carajás-Mineral-Province; Archaean; Granites; Tectonics

* Corresponding author. Tel.: + 33-3-83594234; fax: + 33-3-83511798.
E-mail address: barbey@crpg.cnrs-nancy.fr (P. Barbey).

PII: S0301-9268(00)00103-0

1. Introduction

Tonalites, trondhjemites and granodiorites (TTG) are major components of the Archaean continental crust. Their generation conditions are now fairly well-known from geochemical data (e.g. Barker, 1979; Martin, 1987; Drummond and Defant, 1990; Martin, 1993, 1994) and experimental works (e.g. Johnston and Wyllie, 1988; Rapp, 1991; Rapp and Watson, 1995; see also Johannes and Holtz, 1996, for a review). However, even though some TTG rocks have been clearly characterized as plutons (e.g. Kisters and Anhaeusser, 1995; Collins et al., 1998; Nutman et al., 1999), most are reported as broad orthogneissic domains ('grey gneisses') forming with greenstone sequences a broad dome-and-basin pattern (e.g. Bouhallier et al., 1993; Martin, 1994; Moser, 1994; Choukroune et al., 1997).

In the southeastern part of the Amazonian craton (Marajoara area, Carajás Mineral Province), broad areas of tonalitic and trondhjemitic gneisses have been reported (Docegeo, 1988). In fact, these rocks correspond to plutons emplaced during a deformation event as suggested by Althoff et al. (1993, 1994). They represent, therefore, a good opportunity to study the conditions of emplacement of TTG rocks and their place in the evolution of the Archaean crust. After a summary of our present knowledge of the Archaean evolution of the Carajás Mineral Province, we shall (i) describe the mineralogy, chemistry and structure of the Marajoara granitoids with a special focus on the tonalites, (ii) characterize the strain regime prevailing during their emplacement and consolidation, and compare it with the structural features of the adjacent greenstone belts, and finally (iii) discuss the Archaean structural evolution of the southeastern part of the Amazonian craton in the light of large scale crustal processes invoked for the evolution of the Archaean continental crust (e.g. Choukroune et al., 1995, 1997; Treloar and Blenkinsop, 1995; Collins et al., 1998).

2. Geological setting

The Amazonian craton is exposed in the Guyana and Guaporé shields, situated to the north and the south of the Amazon river, respectively (Fig. 1). It corresponds to a nucleus which remained stable throughout the Neoproterozoic Brasiliano Cycle (Almeida et al., 1981). The Guyana shield consists of minor Archaean high-grade rocks, Palaeoproterozoic greenstone belts (Vanderhaeghe et al., 1998) and medium- to high-grade gneisses and granulites, Mesoproterozoic continental detrital sediments and anorogenic granites (Gibbs and Barron, 1983).

In the Guaporé shield, a wide Archaean domain (3.2–2.5 Ga; review in Macambira and Lafon, 1995) occurs to the southeast in the Carajás Mineral Province. Proterozoic terrains (2.25–0.9 Ga) produced during several episodes of crustal accretion or reworking have also been reported (Teixeira et al., 1989; Sato and Tassinari, 1997). Considered initially as a single Archaean unit (Docegeo, 1988; Araújo et al., 1988, 1994; Souza et al., 1990; Machado et al., 1991; Costa et al., 1995), the Carajás Mineral Province is now regarded as composed of two domains with distinct stratigraphic, tectonic and lithological features (Macambira and Lafon, 1995; Souza et al., 1996b): the Carajás terrain to the north, and the Rio Maria terrain to the south (Fig. 1).

2.1. Carajás terrain

The Archean rocks comprise four main units (Figs. 1 and 2a):

1. An older unit comprising mafic to felsic granulite-facies rocks (Pium Complex) dated at 3050 ± 114 Ma (whole-rock Pb–Pb data from felsic granulites; Rodrigues et al., 1992), and undifferentiated tonalitic to granodioritic gneisses and migmatites (Xingu Complex; Silva et al., 1974; Araújo and Maia, 1991), with ages at 2859 ± 2 and 2851 ± 4 Ma (zircon U–Pb data; Machado et al., 1991).
2. Metavolcanics and metasediments (Itacaiúnas supergroup) subdivided into three groups: Grão Pará, Salobo and Pojuca. The Grão Pará Group is composed of bimodal volcanics and iron formations overlain by basic metavolcanics and metasediments containing Mn (Azul deposit), Au–Cu (Bahia deposit) and Au–Pt (Serra Pelada) deposits (Beisiegel

et al., 1973; Gibbs et al., 1986; Docegeo, 1988). Metarhyolites from the lower part of the Grão Pará Group are dated at 2759 ± 2 Ma (zircon U–Pb data; Machado et al., 1991). The Salobo and Pojuca Groups are composed of metabasalts, iron formations and clastic sediments containing Cu, Au, Ag, Mo mineralizations (Docegeo, 1988; Lindenmayer et al., 1995). Intrusive alkaline granites (Plaquê Suite; Araújo et al., 1988) emplaced in the undifferenciated Xingu Complex at 2747 ± 2 Ma (zircon Pb–Pb; Huhn et al., 1999) and 2729 ± 29 Ma (zircon Pb–Pb; Avelar, 1996).

3. The Aguas Claras Formation, overlaying the Itacaiúnas supergroup, is composed of mudstones, siltstones and sandstones (Araújo et

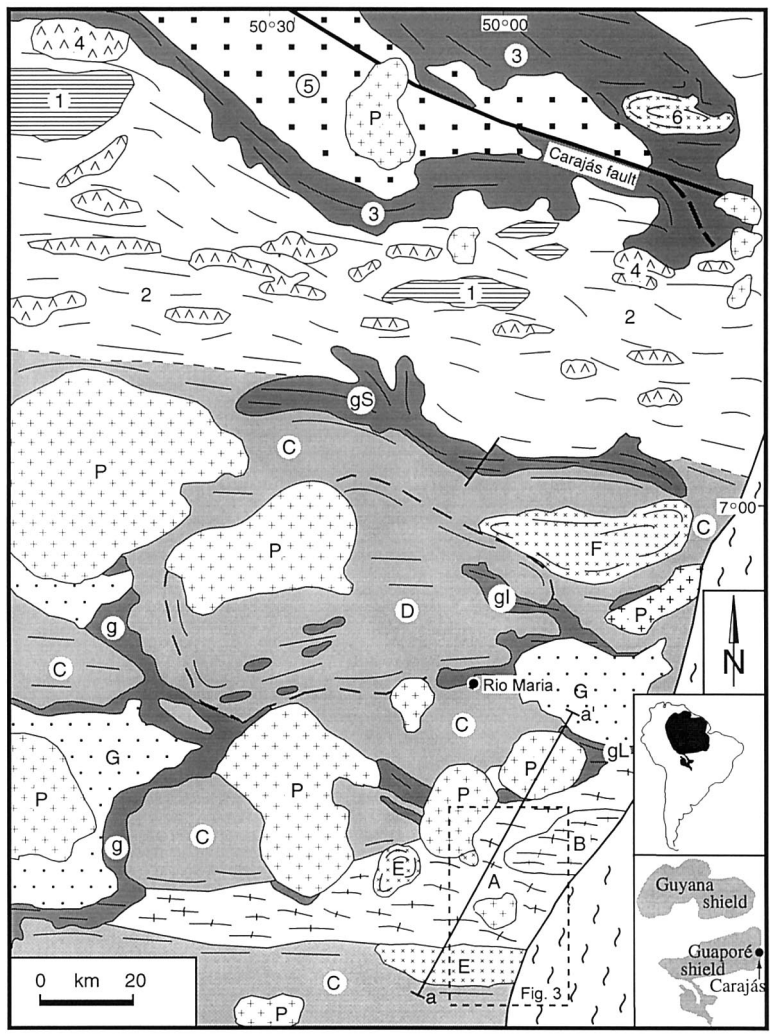

Fig. 1. Geological sketch maps of the Carajás Mining province redrawn from Araújo et al. (1988), Docegeo (1988), Souza et al. (1990). Carajás terrain: (1) Pium Complex, (2) Xingu Complex, (3) Itacaiúnas supergroup, (4) Plaquê Suite, (5) Aguas Claras Formation, (6) Estrela Granite Complex; Rio Maria terrain: (g) Andorinhas supergroup (gS, Sapucaia; gI, Identidade; and gL, Lagoa Seca and Babaçu greenstones), (A) Arco Verde Tonalites, (B) Guarantã monzogranite, (C) Rio Maria Granodiorites, (D) Mogno Trondhjemites, (E) Mata Surrão Monzogranites, (F) Xinguara Granite, (G) Rio Fresco Group and (P) Palaeoproterozoic Granites. aa′ = cross-section of Fig. 2.

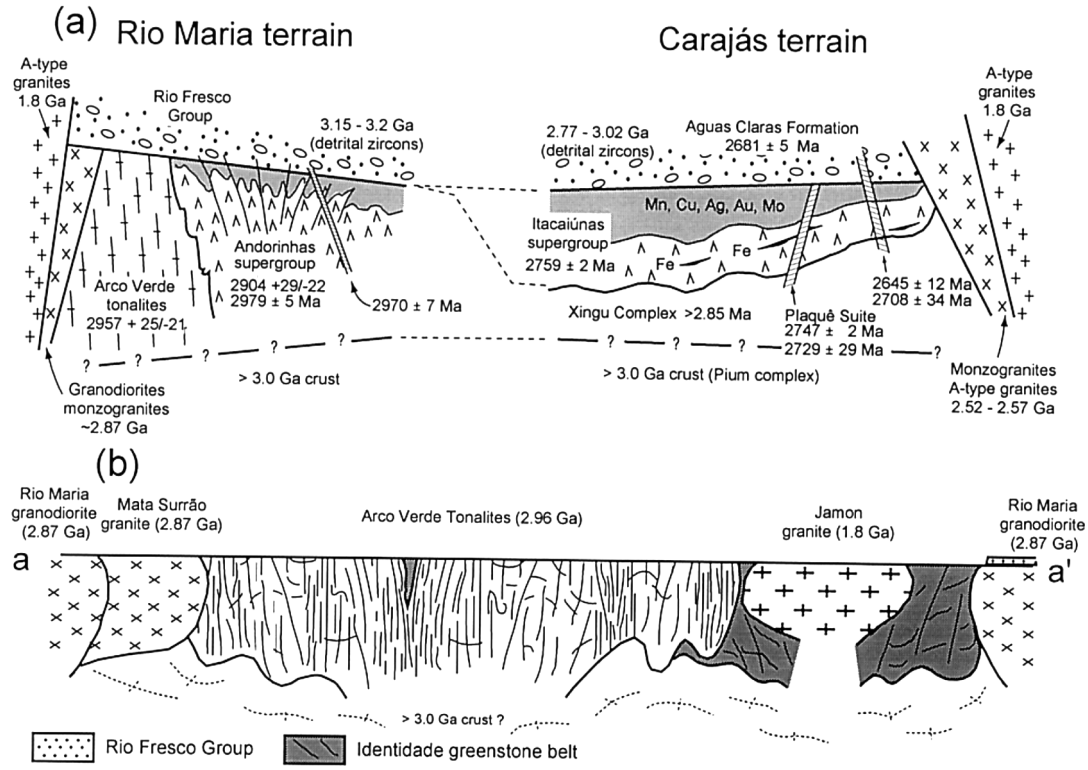

Fig. 2. (a) Compared lithostratigraphic successions of the Carajás and Rio Maria terrains; and (b) interpretative cross-section of the Marajoara area (location given in Fig. 1).

al., 1988). Detrital zircons from this formation yielded ages ranging from 2.77 to 3.02 Ga (zircon U–Pb data; Mougeot, 1996), whereas zircons considered to be derived from syndepositional volcanism are dated at 2681 ± 5 Ma (zircon U–Pb; Trendall et al., 1998). The Aguas Claras formation is cut by sills and dikes of gabbro and diabase, with zircon U–Pb crystallization ages of 2708 ± 37 (Mougeot, 1996) and 2645 ± 12 Ma (Dias et al., 1996).

4. The Archaean evolution ended with the emplacement, in the Itacaiúnas supergroup, of monzogranites (Itacaiúnas granite, 2560 ± 37 Ma; zircon Pb–Pb data; Souza et al., 1996a) and A-type granitoids as the Estrela granite complex (2527 ± 68 Ma; whole-rock Rb-Sr isochron; Barros et al., 1992, 1997) and the Old Salobo granite (2573 ± 2 Ma; zircon U–Pb data; Machado et al., 1991).

2.2. Rio Maria terrain

It corresponds to a 2.87–3.2 Ga granite–greenstone assemblage (Figs. 1 and 2a) locally overlain by a ~ 2 km-thick, clastic sedimentary cover (Rio Fresco Group; Docegeo, 1988). Evidence of a pre-3.0 Ga crust is attested in the Rio Maria area by 3.15 and -3.2 Ga zircons found in the Rio Fresco sediments and in the 1.8 Ga Musa granite (Macambira and Lancelot, 1991; Machado et al., 1991). The greenstone sequence (Andorinhas Supergroup) is composed chiefly of komatiites and tholeiitic basalts. Felsic metavolcanics occurring in the upper stratigraphic unit (Lagoa Seca Group; Cordeiro and Saueressig, 1980) have been dated at $2904 + 29/-22$ Ma (zircon U–Pb data; Macambira and Lancelot, 1992, 1996) and at 2979 ± 5 Ma (zircon U–Pb data; Pimentel and Machado, 1994). In the south, the Andorinhas

greenstones are cut by a sill of ultramafic rocks (Serra Azul complex; Docegeo, 1988) with a crystallization age of 2970 ± 7 Ma (zircon U–Pb; Pimentel and Machado, 1994). Granitoids form plutonic belts alternating with greenstones. In the Marajoara area they comprise:

1. the Arco Verde tonalites (Althoff et al., 1993, 1994), a typical tonalite-trondlijemitediorite suite with an emplacement age of 2957 + 25/ − 21 Ma (zircon U-Pb; Macambira and Lancelot, 1996), similar within errors to that of the greenstones; and
2. various calc-alkaline and potassic granitoids (Medeiros et al., 1987; Docegeo, 1988; Duarte et al., 1991; Althoff et al., 1993) with ages ranging from 2.93 to 2.85 Ga, namely: the Guarantã monzogranite (2.93 Ga; zircon U–Pb; Macambira, Personal communication, 1999), the Rio Maria granodiorites dated at 2874 + 9/ − 10 Ma (zircon U–Pb; Macambira and Lancelot, 1991, 1996) and 2872 ± 5 Ma (zircon and titanite U–Pb; Pimentel and Machado, 1994), the Mata Surrão monzogranites dated at 2872 ± 10 Ma (whole-rock Pb–Pb data; Lafon et al., 1994) and 2871 ± 7 Ma (zircon Pb–Pb; Althoff et al., 1998), the Mogno trondhjemite (2871 Ma, titanite Pb–Pb data; Pimentel and Machado, 1994), and the Xinguara granite (2.8-2.88 Ga; zircon U–Pb; Macambira et al., 1991). Similar Pb–Pb ages (2872 ± 25 Ma) have also been reported for granitoids from Redenção, to the south of the area studied (Barbosa and Lafon, 1996).

To summarize, the evolution of the Archaean crust in the Carajás Mineral Province occurred in four main stages: 3.2–3.0 Ga (underlying crust), 2.98–2.93 Ga (greenstones and TTG), ca. 2.87 Ga (calc-alkaline granitoids), and 2.75–2.55 Ga (volcanic and detrital sedimentary sequences, and late granites). Although the Rio Fresco Group and Aguas Claras Formation are likely to belong to a same clastic sedimentary cover, and although the undifferentiated Xingu Complex can be considered as equivalent to the calc-alkaline granites of the Rio Maria terrain, we emphazise the following points:

1. The Andorinhas supergroup (2.97–2.90 Ga) and the related TTG rocks (2.96 Ga), occur only in the Rio Maria terrain and correspond to a typical granite–greenstone association.
2. The Itacaiúnas supergroup (2.76 Ga) and its related mineralizations are restricted to the Carajás terrain. The presence of 2.76 Ga continental-type sequences only in the Carajás terrain seems to be attributed to a distinct geotectonic environment (Araújo et al., 1988) rather than to distinct erosion levels.
3. Sheeted alkaline granites (2.75 Ga) and A-type granites (2.57 Ga) seem to be restricted to the Carajás terrain.

A common evolution of both the Rio Maria and Carajás terrains is attested only from the Palaeoproterozoic, by 1.8 Ga anorogenic granites which occur in both terrains (review in Dall'Agnol et al., 1994).

3. Lithology and chemistry

The Marajoara area covers ∼900 km in the southern part of the Rio Maria terrain (Fig. 1). Although discontinuous, granitoid outcrops are rather good compared with those found elsewhere in the craton. This study deals mainly with the Arco Verde tonalites, and to a lesser extent with the Guarantã and Mata Surrão monzogranites, and with the Rio Maria granodiorites (Figs. 2b and 3). Fourty-four samples from these units were analyzed for major and trace elements. Modal compositions are given in Fig. 4, and representative whole-rock analyses in Tables 1 and 2.

3.1. Arco Verde tonalites (2.96 Ga)

The Arco Verde tonalite (AVT) unit is the oldest and consists of grey, equigranular, medium-grained (locally fine-grained) tonalites and trondhjemites with igneous isotropic to strongly foliated textures. Widespread compositional banding is defined by layers of distinct modal compositions, indicating mingling of crystal-rich magmas with distinct proportions of biotite and feldspars. Quartz-dioritic microgranular enclaves (10–80 cm in length) are common. Conformable or cross-cutting veins of aplites and pegmatites are widespread. Exceptionally, one

hectometre-sized enclave of recrystallized metapelites has been found in the Arco Verde tonalites to the south-east of Marajoara. This enclave shows evidence of intense recrystallizations due to contact metamorphism, superimposed on an early low-grade phase assemblage associated with a schistosity. Small euhedral limpid zircons from this enclave yielded a 2927 ± 24 Ma age (SHRIMP U–Pb; Althoff et al., 1997, 1998). Although younger, this age cannot be distinguished within uncertainties from that of the tonalites ($2957 + 25/-21$ Ma). Contacts between the AVT and the surrounding greenstone belts are concealed by younger intrusions, or not exposed.

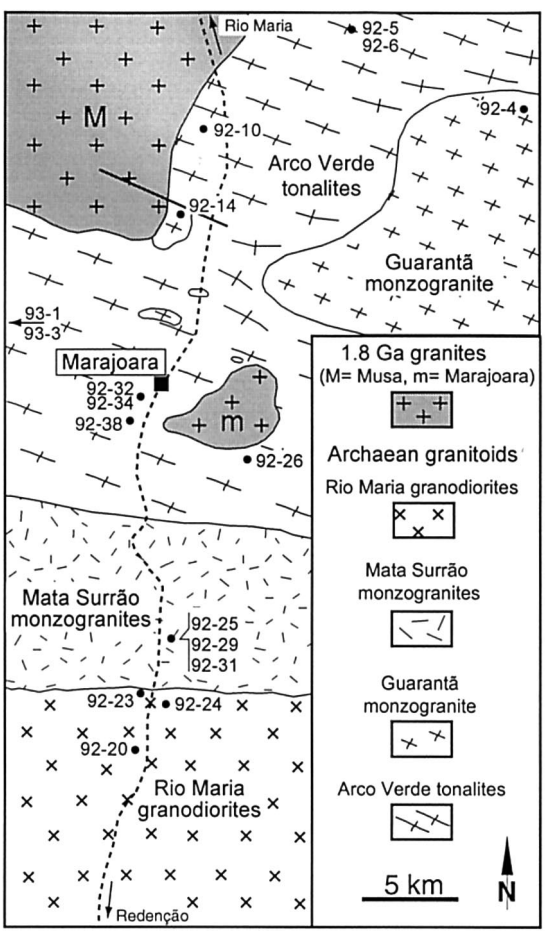

Fig. 3. Geological sketch map of the Marajoara area. Numbers refer to sample analyses of Tables 1 and 2.

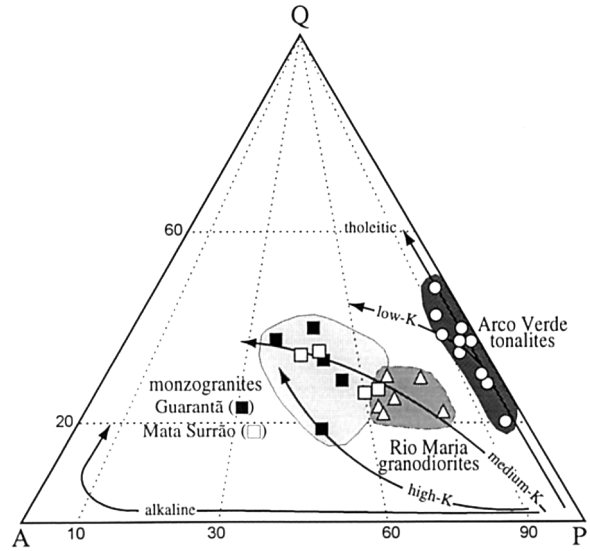

Fig. 4. QAP plot of modal compositions of the Marajoara granitoids. Tholeiitic, calc-alkaline and alkaline differentiation trends are also shown.

The Arco Verde tonalites are composed essentially of plagioclase (An_{22-33}; 44–64%) and quartz (17–44%), with more restricted microcline ($Or_{94-98}An_0$; < 5%) and biotite ($X_{Mg} = 0.50–0.63$; 3–13%). Plagioclases generally display a faint chemical zonation (An < 2%), but albitic rims are common. Amphibole (pargasitic and edenitic hornblende; $X_{Mg} = 0.37–0.49$) is rare, except in the contact aureoles around the younger Palaeoproterozoic granites where it appears in association with magnetite (rare clinopyroxene), as centimetre-sized poikiloblastic crystals including recrystallized quartz and feldspars grains. Accessories are titanite, apatite, zircon, allanite, magnetite, ilmenite and pyrite (rare chalcopyrite). Secondary minerals are chlorite, carbonates, epidote, sericite, hematite and goethite (Magalhães et al., 1994).

In normative An–Ab–Or or Qz–Ab–Or diagrams, the Arco Verde tonalite samples ($64 < SiO_2 < 73\%$; average $K_2O/Na_2O = 0.54$; $Mg\# = 0.33$) follow the trend of low-K suites with Na enrichment. The Al_2O_3 contents range from 13.5 from 13.5 to 17%, but are < 15% at $SiO_2 = 70\%$, a characteristic of the low-alumina trondhjemites (Barker and Arth, 1976). Major-

Table 1
Major (wt.%) and trace element (ppm) composition of the Arco Verde tonalites[a]

	Sample no.								
	92-6	92-5	92-34	92-26	92-10	93-1	92-38	92-32	93-3
SiO_2	66.43	67.12	68.9	69.43	70.54	71.7	72.06	72.54	72.78
Al_2O_3	15.43	16.35	15.53	15.38	14.55	14.47	14.26	14.31	14.83
Fe_2O_3[b]	3.64	3.59	3.59	3.54	3.0	2.59	2.24	2.04	1.05
MnO	0.04	0.03	0.03	0.04	0.05	0.04	0.03	0.02	–[c]
MgO	1.04	0.97	0.91	0.79	0.75	0.61	0.48	0.4	0.31
CaO	3.12	3.33	3.77	3.2	2.52	2.56	2.16	2.16	1.67
Na_2O	5.99	4.58	4.5	4.8	4.16	4.04	4.3	4.0	4.91
K_2O	2.15	2.33	1.29	1.38	3.12	2.67	3.12	3.45	3.36
TiO_2	0.4	0.34	0.34	0.32	0.29	0.27	0.19	0.17	0.12
P_2O_5	0.22	0.13	0.17	0.15	0.11	0.11	0.08	0.08	0.02
L.O.I.	0.77	0.87	0.72	0.74	0.4	0.66	0.83	0.56	0.63
Total	99.23	99.64	99.75	99.77	99.49	99.72	99.75	99.73	99.68
Ba	965	1142	269	234	848	766	528	770	887
Co	6	7	4	3	6	4	2	1	1
Cr	11	10	2	2	13	6	2	5	5
CU	18	9	1	–	7	3	5	–	3
Nb	4	6	6	14	7	10	9	7	9
Pb	8	11	9	11	10	13	14	15	24
Rb	63	63	85	76	113	133	104	125	227
Sc	5	3	5	5	4	4	3	3	3
Sr	838	432	317	255	347	188	187	227	336
Th	4	16	11	16	7	13	9	9	7
U	1	1	2	2	1	2	1	1	9
V	46	29	18	11	34	15	8	4	11
Y	5	5	8	9	9	18	6	5	9
Zn	47	56	58	75	51	55	55	39	23
Zr	129	147	218	239	132	129	127	112	66
La	30.9	48.8	44.6	62.0	30.2	34.7	22.2	23.5	10.4
Ce	64.1	92.1	76.7	109.1	56.8	63.0	42.3	43.6	19.2
Pr	6.9	9.1	7.2	10.5	5.5	6.4	4.1	4.1	2.4
Nd	26.0	29.2	23.6	34.6	18.3	22.5	14.2	14.1	8.7
Sm	4.0	4.0	3.1	5.1	2.9	3.9	2.6	2.2	1.7
Eu	1.1	1.0	0.8	0.9	0.8	0.9	0.6	0.6	0.5
Gd	2.7	2.7	2.3	3.8	2.3	3.0	2.0	1.8	1.3
Th	0.3	0.3	0.3	0.4	0.3	0.4	0.3	0.2	0.2
Dy	1.2	1.1	1.4	2.0	1.5	2.8	1.3	1.0	1.1
Ho	0.2	0.2	0.3	0.3	0.3	0.5	0.2	0.2	0.3
Er	0.4	0.5	0.7	0.8	0.8	1.5	0.5	0.4	0.7
Tm	0.1	0.1	0.1	0.1	0.1	0.2	0.1	0.1	0.1
Yb	0.4	0.4	0.7	0.7	0.8	1.6	0.5	0.4	1.0
Lu	0.1	0.1	0.1	0.1	0.1	0.2	0.1	0.1	0.2

[a] Major elements and Sc concentrations were determined by ICP-AES, and trace elements by ICP-MS at CRPG-CNRS (Nancy). Analytical uncertainties are estimated at 2% for major elements, and at 5 or 10% for trace-element concentrations (except REE) higher or lower than 20 ppm, respectively. Precision for REE is estimated at 5% when chondrite-normalized concentrations are >10 and at 10% when they are lower.

[b] Fe_2O_3 is the total iron.

[c] Below detection limit. The full data set is available on request.

Table 2
Representative major (wt.%) and trace (ppm) element analyses of the Guarantã, Mata Surrão and Rio Maria granitoids[a]

	Guarantã monzogranites		Mata Surrão monzogranites			Rio Maria granitoids		
	92-4	92-14	92-29	92-31	92-25	92-20	92-23	92-24
SiO_2	71.34	72.9	71.24	72.56	72.92	63.03	64.5	67.15
Al_2O_3	14.98	12.73	14.96	14.58	13.76	15.11	15.5	16.07
Fe_2O_3[b]	1.79	5.44	1.61	1.13	1.91	5.44	3.97	3.08
MnO	–[c]	0.02	0.02	0.02	0.02	0.08	0.06	0.03
MgO	0.56	2.12	0.39	0.29	0.48	3.5	2.22	0.96
CaO	1.72	0.3	1.37	1.43	1.54	4.62	3.12	2.72
Na_2O	5.05	3.47	4.62	4.75	4.24	4.04	4.66	5.34
K_2O	3.02	1.52	4.72	3.94	3.79	2.97	2.87	2.27
TiO_2	0.17	0.76	0.29	0.12	0.13	0.44	0.43	0.4
P_2O_5	0.12	0.17	0.12	0.07	0.06	0.2	0.19	0.17
L.O.I.	0.86	0.32	0.95	0.8	0.9	0.99	1.13	1.45
Total	99.61	99.75	100.29	99.69	99.75	100.42	98.65	99.64
Ba	1375	1464	1722	1056	763	966	859	856
Co	3	67	1	4	2	21	13	5
Cr	9	–	–	29	5	135	132	12
CU	13	9	1	5	2	47	28	4
Nb	3	8	5	13	16	8	13	7
Pb	10	13	25	25	17	11	14	14
Rb	68	227	142	138	123	130	112	87
Sc	3	11	2	3	4	12	7	4
Sr	639	100	665	577	318	564	719	666
Th	3	7	22	15	12	5	11	7
U	1	2	4	9	11	1	7	2
V	17	–	7	18	11	87	58	33
Y	5	10	3	8	15	17	21	8
Zn	21	13	37	36	33	58	85	58
Zr	102	57	201	95	81	115	161	141
La	16.4	10.6	62.5	20.2	16.5	31.7	51.8	34.0
Ce	33.5	20.5	113.5	38.9	33.1	66.8	64.7	64.6
Pr	3.5	2.1	10.8	4.0	3.4	7.3	9.2	6.9
Nd	13.3	7.2	33.2	14.8	12.5	26.4	33.9	25.3
Sm	2.2	1.3	4.0	2.5	2.3	4.0	6.1	3.8
Eu	0.8	0.6	1.0	0.8	0.5	1.0	1.5	1.0
Gd	1.7	1.2	2.4	1.8	2.1	3.2	5.1	2.9
Th	0.2	0.2	0.2	0.2	0.4	0.4	0.7	0.4
Dy	1.1	1.3	0.9	1.3	2.0	2.2	3.4	1.6
Ho	0.2	0.3	0.1	0.3	0.5	0.5	0.7	0.3
Er	0.5	1.0	0.3	0.6	1.3	1.2	1.5	0.7
Tm	0.1	0.2	0.0	0.1	0.2	0.2	0.2	0.1
Yb	0.4	1.3	0.2	0.6	1.5	1.3	1.3	0.7
Lu	0.1	0.2	0.0	0.1	0.3	0.2	0.2	0.1

[a] See Table 1 for analytical techniques.
[b] Fe_2O_3 is the total iron.
[c] Below detection limit.

element variation diagrams (e.g. TiO_2–SiO_2; Fig. 5a) show that the AVT samples define differentiation trends consistent with fractional crystallization. The behaviour of compatible (Co, Cu, Sr, V) and incompatible (Pb, Rb) trace-elements corroborate the role of fractional crystallization in the

differenciation of the Arco Verde tonalites (e.g. Rb–Sr; Fig. 5b). However, the lack of correlation of Eu/Eu* ratios (≥ 0.9 for most of them) with differentiation index strongly suggest that the samples studied are not representative of melts but corresponded to a mixture of melt and cumulate minerals. This is also supported by the presence of feldspar- or biotite-enriched layers suggesting crystal accumulation. Rb/Sr ratios in the AVT (0.39 on average) are similar to the average continental crust (0.32; Taylor and McLennan, 1985), but are significantly higher than those in the TTG suites (0. 15, Condie, 1993). This may correspond to post-crystallization modifications, as suggested by Macambira et al. (1991), Lafon et al. (1994) from isotopic data indicating opening of the Rb–Sr system at $\sim$ 2.5–2.6 Ga. Chondrite-normalized REE concentrations are variable ($41 < La_N < 134$, $2.1 < Yb_N < 14.3$), but the patterns (Fig. 5c) are always strongly fractionated (average $La/Yb_N = 37$) with concave upwards HREE and small or no Eu

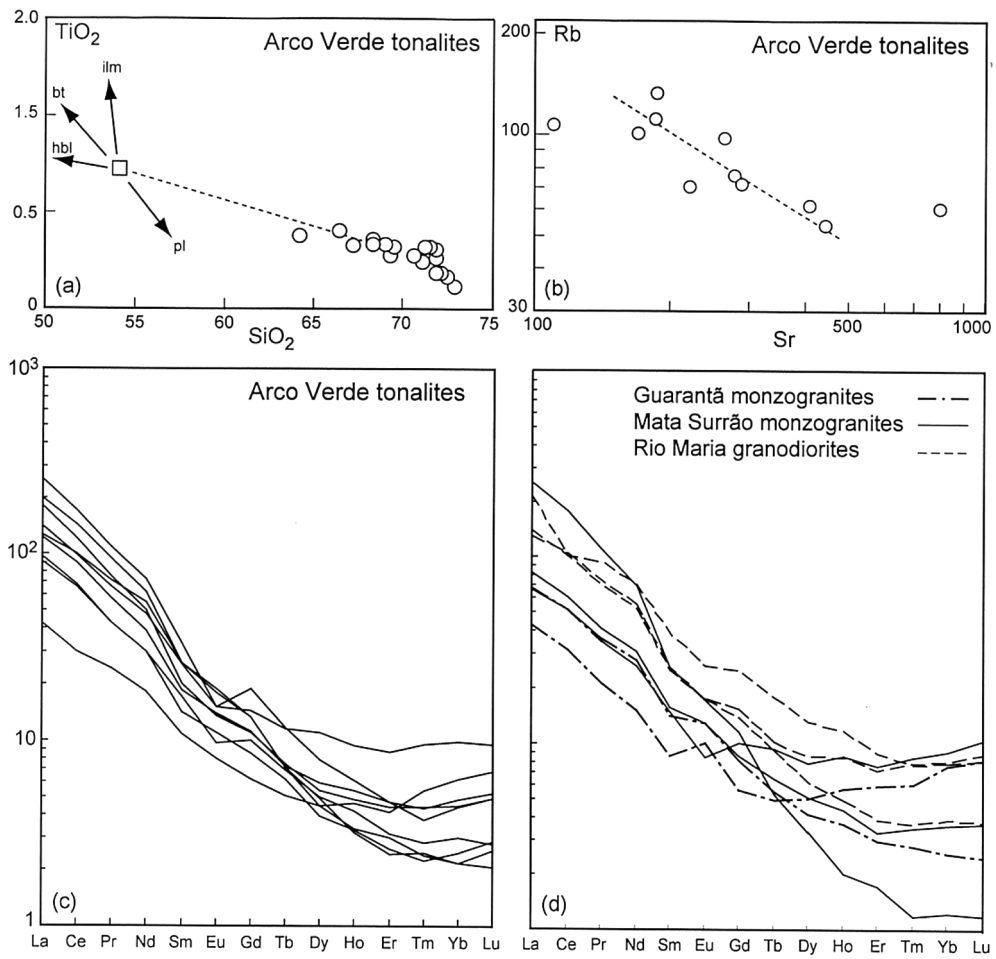

Fig. 5. Major- and trace-element composition of the granitoids of the Marajoara area: (a) TiO_2–SiO_2 plot for the Arco Verde tonalites (○) showing a differentiation trend consistent with fractional crystallization involving a residue (□) composed of plagioclase, hornblende, biotite and ilmenite; (b) Rb–Sr plot for Arco Verde tonalites; (c) and (d) chondrite-normalized REE patterns for the Arco Verde tonalites, Guarantã and Mata Surrão monzogranites and Rio Maria granodiorites (normalization values from Evensen et al., 1978).

anomaly ($0.60 < Eu/Eu^* < 1.07$). Average Yb content (0.89 ppm) are close to that of the mean Archaean TTG rocks (Yb = 1 ppm; Condie, 1993).

Mass-balance calculations involving SiO_2, Al_2O_3, MgO, CaO and TiO_2, show that the differentiation trends of the AVT are consistent with fractional crystallization of plagioclase, hornblende, biotite and ilmenite in 70/24/5/1 proportions. Except for small amounts of biotite, this composition is not significantly different from that reported by Martin (1987) for the Archaean TTG from eastern Finland. The amount of crystallization cannot have exceeded 30%. The fractionated concave-upward REE patterns with low Yb contents further show that the parental melts may have been in equilibrium with a gamet-hornblende-bearing solid residue (10–25% garnet).

3.2. The younger granites (2.93-2.87 Ga)

Three main bodies of calc-alkaline and potassic granitoids crosscut the Arco Verde tonalites in the area studied (Fig. 3): they correspond to the Guarantã and Mata Surrão monzogranites and to the Rio Maria granodiorites.

The Guarantã monzogranite (2.93 Ga) is strongly deformed and consist of foliated coarse-grained porphyritic pink granites with a well-developed mineral lineation. The Mata Surrão monzogranites (2.87 Ga) originally described to the west of Marajoara (Duarte et al., 1991), are deformed weakly and consist of medium-grained equigranular grey granites. Decimetre-sized, fine-grained, microdioritic enclaves are locally found in both units. Crosscutting veins of granite, pegmatites and diorites are common. Monzogranites consist mainly of plagioclase (22–50%), K-feldspar (20–55%) and quartz (19–35%), with a few percents of biotite ($X_{Mg} = 0.49–0.59$). Plagioclase comprises subhedral crystals ($An_{12–18}$) and recrystallized grains ($An_{2–4}$). K-feldspar is a perthitic ($Or_{79–86}An_0$) microcline ($Or_{95–97}$). Accessories are magnetite, apatite, titanite, zircon, allanite, and garnet. Secondary assemblages comprise sericite, chlorite, epidote and carbonates.

In the Marajoara area, the granodiorites display the same mineralogical, chemical and structural characteristics as the Rio Maria granodiorite which was originally described farther north, near the Rio Maria locality (Medeiros et al., 1987). The granodiorites are greenish grey, equigranular, medium-grained rocks, dominantly isotropic although a weak planar fabric is observed locally. They contain centimetre-sized, rounded to slightly flattened, mafic microgranular enclaves consisting of andesine, hornblende and biotite, and are cut across by pegmatites and quartz veins. The granodiorites consist of plagioclase ($An_{29–40}$; 37–53%), microcline ($Or_{94–96}An_0$; 10–19%) and quartz (18–25%). Plagioclase zonation can be oscillatory, but more commonly normal (An core-rim variations reaches 7%). Amphibole ($X_{Mg} = -0.60$; 8–19%) is slightly more abundant than in the granodiorites from Rio Maria (-6%). Its composition ranges from hornblende, mainly, to actinolite according to Leake et al.'s (1997) classification. Biotite ($X_{Mg} = -0.45$; 2–7%) occurs in addition to amphibole. Accessory phases are apatite, oxides, zircon and titanite. Secondary assemblages comprise chlorite, sericite, apatite, epidote, and clay minerals.

The monzogranites ($70 < SiO_2 < 76$%; average $K_2O/Na_2O = 0.8$; $Mg\# = 0.37$) and granodiorites ($62 < SiO_2 < 69$%; average $K_2O/Na_2O = 0.76$; $Mg\# = 0.52$) follow the calc-alkaline differentiation trend (Fig. 4). The Guarantã and Mata Sur-rão monzogranites display similar REE concentrations (Fig. 5d) with fractionated patterns and generally low Yb contents ($5.6 < La/Yb_N < 211$; $1.2 < Yb_N < 9.1$). The Rio Maria granodiorites display major-element compositions similar to high-Mg granodiorites. They have fractionated patterns (Fig. 5d) with low Yb contents and a weak negative Eu anomaly (average $La/Yb_N = 26$; $0.6 < Yb < 1.3$ ppm; $Eu/Eu^* \geq 0.84$).

4. Structural data

The Rio Maria terrain displays the typical dome-and-keel structures (Fig. 1) of the granite-greenstone terrains world-wide. The main structural element in the Marajoara region is a WNW–ESE subvertical foliation. It is well developed in the Arco Verde tonalites and in the Guarantã monzogranite, but absent in the Mata

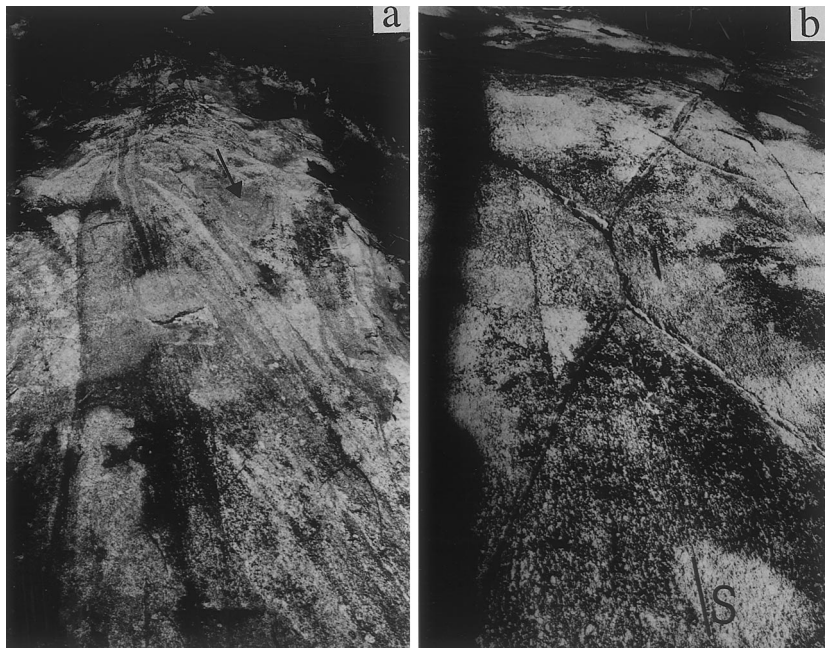

Fig. 6. Synmagmatic and subsolidus structures of the Arco Verde Tonalites: (a) subvertical cross-layering and folded layering with horizontal axis (arrowed), observed in low strain domains; (b) orthogneissic tonalite with a subvertical foliation outlined by quartz ribbons and crosscut by conjugated brittle zones filled with quartz.

Surrão monzogranite and in the Rio Maria granodiorites.

4.1. Arco Verde tonalites

At the outcrop scale, low-strain domains are close to highly-deformed, foliated domains. The foliation is defined by alternate cm- to dm-thick tonalitic to trondhjemitic bands. It trends N100–120°E (except for limited local variations), generally with a steep dip to north or south. It corresponds to a single deformation plane (*XY* plane of the finite strain ellipsoid), but developed within a large temperature range, from magmatic to subsolidus low-T conditions. Layering can be continuous for several hundred metres, but is more commonly disturbed by cross-layering (Fig. 6a), pinch-and-swell structures, and crosscut by synmagmatic vertical shear zones, veins and tension gashes. The foliation is defined by the preferred orientation of biotite, feldspars and flattened polycrystalline quartz aggregates (Fig. 6b). In domains of high deformation, the compositional layering is accompanied by a well-developed near vertical foliation, and mafic enclaves are strongly flattened. The foliation (high-T mylonites in zones of high strain) is commonly parallel to the layering but is always axial planar for the folds. The mineral or stretching lineation, when clearly expressed, is always subhorizontal and outlined by elongated quartz grains displaying microstructures suggesting high- to medium-T recrystallization. In low-strain domains in the centre of the massif near the locality of Marajoara, a horizontal layering is locally preserved (Fig. 6a). It is disturbed by synmagmatic upright tight folds with WNW–ESE trending subhorizontal axes. In this case, tonalites preserve equigranular magmatic structures (Fig. 7a) with euhedral zoned plagioclases and interstitial quartz with limited intracrystalline deformation (undulatory extinction or slight recrystallisation).

The mafic microgranular enclaves are oriented parallel to the foliation and never show sigmoldal structures, but may display high axial ratios (10:3–80:3 in the *XZ* plane, less important but still high in the *YZ* plane).

Metre- to decametre-long shear-zones (locally filled with pegmatite, aplite or quartz) are common in zones of intense deformation. They are vertical or steeply inclined, with a subhorizontal sense of displacement, and occur either in single or conjugated sets, with sinistral or dextral senses of displacement. Conjugated shear-zones make variable angles (Fig. 8) depending on their nature (syn-magmatic, ductile or brittle), ranging from 20° in high-T magmatic domains to 90° in low-T domains. But the acute bissectrix of this angle always corresponds to the planar fabric (Fig. 6b). These increasing angle variations suggest that the shear-zones developed under decreasing temperatures, i.e. during pluton emplacement and cooling. This is also consistent:

1. with microstructures which display a transition from the magmatic stage (euhedral to subhedral crystals, weak intracrystalline deformation; Fig. 7a) to subsolidus stages at high-T (ductilly deformed quartz and feldspars; Fig. 7b), middle-T (ductilly deformed quartz, brittle feldspars; Fig. 7c) and low-T (cataclasis); and
2. with mineral assemblages consisting of either plagioclase + quartz + biotite ± hornblende in synmagmatic to subsolidus high-T foliation and ductile shear-zones, or plagioclase + quartz + biotite ± muscovite in medium-T structures, or epidote + chlorite + albite + quartz in low-T brittle zones.

Non rotational strain is suggested by the nature and position of the veins and tension gashes with respect to the foliation: veins (filled with aplite, pegmatite or quartz) parallel to the foliation are boudinaged, whereas those at high-angle with it are folded; tension gashes (quartz-bearing) are perpendicular to the foliation.

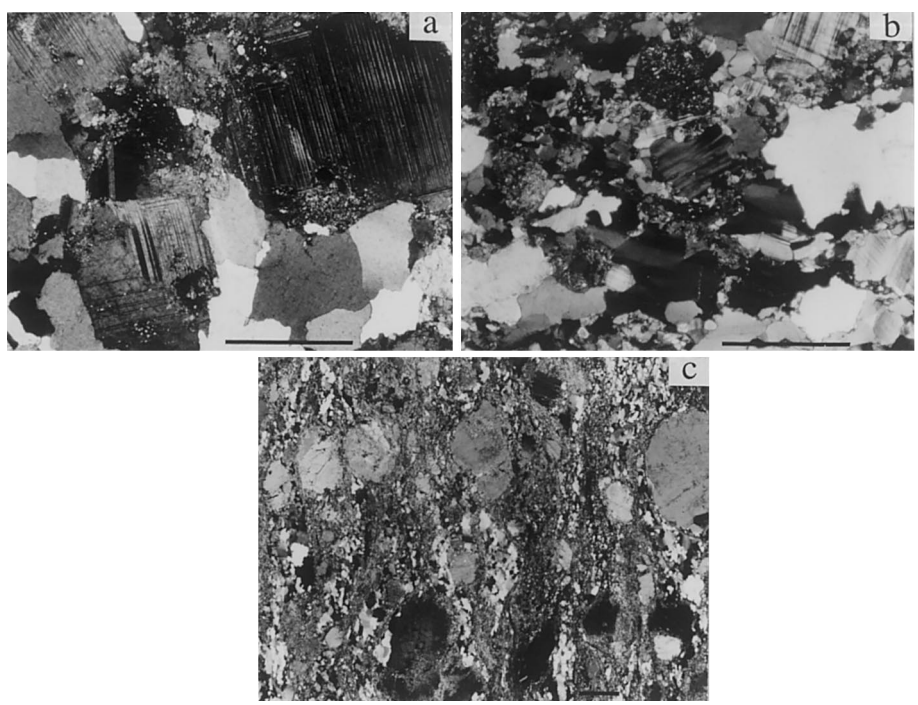

Fig. 7. Microstructures in the Arco Verde Tonalites: (a) magmatic assemblage with subhedral slighly zoned plagioclase and interstitial quartz; (b) subsolidus high-T microstructures with recrystallized feldspars and quartz; (c) microstructures in a medium- to low-T shear zone in the tonalites (the fine-grained matrix consists of quartz, plagioclase, biotite and muscovite).

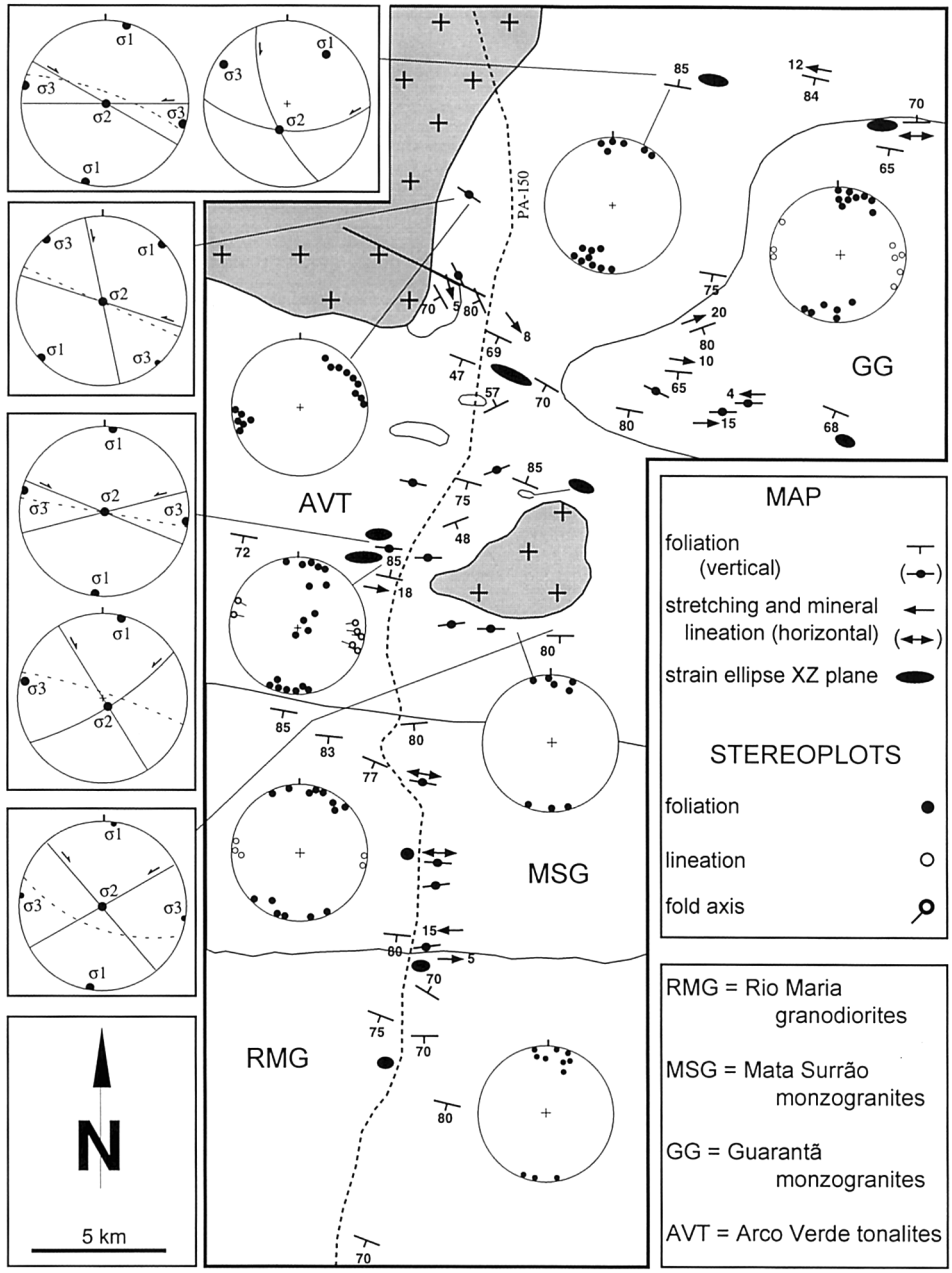

Fig. 8. Stereographic projections of the symnagmatic to subsolidus structures of the Arco Verde Tonalites, and inferred σ_1, σ_2, σ_3.

4.2. Monzogranites and Rio Maria granodiorites

The Guarantã monzogranite crosscut the Arco Verde unit, but no thermal effects are observed in the tonalites near the contacts. Magmatic structures (euhedral zoned crystals, porphyritic textures, magma mingling) are rare, due to intense subsolidus, dominantly high-temperature, deformation. Nevertheless, medium- to low-temperature microstructures are also observed. A

widespread and well-developed WNW–ESE trending subvertical foliation is associated to a subhorizontal stretching lineation. These structures are outlined by the preferred orientation of biotite, feldspar megacrysts and quartz ribbons. The foliation in the Guarantã monzogranite is parallel to that in the Arco Verde tonalites, and the lineation trends parallel to fold axes of tonalites. Some E–W trending subvertical centimetre-thick ductile shear zones are observed. Recrystallized tails in feldspars are symmetric or show preferentially a dextral sense of shear, also indicated by oblique schistosity in mafic dykes conformable with the granite foliation.

The Mata Surrão monzogranites and the Rio Maria granodiorites are almost undeformed. In the latter, flow structures are scarcely observed and mafic microgranular enclaves are generally rounded. However, a weak E–W trending subvertical fabric is locally visible by the preferred orientation of hornblende and weakly flattened mafic enclaves. In thin sections weakly recrystallized quartz and undulose extinction in feldspars are observed.

4.3. Finite strain data

To examine the nature of the finite strain in the granitoids from Marajoara, axial ratios of strain ellipsoids were determined by digitalization of perimeters of quartz and feldspars in oriented thin sections from representative samples. Measurements were made with a videographic analyser and axial ratios obtained using the method of Panozzo (1984) modified by Lapique et al. (1988). The Arco Verde tonalites and Guarantã monzogranite are the most deformed. The strain ellipsoids are in most cases oblate, especially when measured using quartz aggregates ($X/Y-1.\ 5$; $2<Y/Z<3$), suggesting that both units were submitted to flattening, related to the bulk of the regional deformation. However, prolate strain ellipsoids of constrictional type occur into local minor shear zones and for feldspars measured in low-T deformed rocks ($1<X/Y<2$; $Y/Z<0.5$). In the Rio Maria granodiorite (both at Rio Maria and Marajoara), strain ellipsoids display axial ratios close to unity, indicating either a very weak deformation, or a magmatic foliation. However, these axial ratios close to 1 does not allow the type of deformation to be specified, because the shape of crystals may be of magmatic origin (euhedral feldspars) or imposed by the neighbouring grains (interstitial quartz).

5. Discussion

The granitoids in the Marajoara area consist mainly of two magmatic series emplaced in two distinct episodes: one of trondhjemitic affinity emplaced syntectonically at ca. 2.96 Ga (Arco Verde Tonalites), and the other of calc-alkaline affinity emplaced post-tectonically 100 Ma later at ca. 2.87 Ga (Mata Surrão monzogranites and Rio Maria granodiorites).

5.1. Structure of the granitoids and the local deformation

A locally penetrative, subvertical, N100–110E-trending foliation is well developed in the Arco Verde tonalites and in the Guarantã monzogranite, but mostly absent in the younger Mata Surrão monzogranites and Rio Maria granodiorites. The lineation, when clearly expressed, is a subhorizontal, high- to medium-T, stretching or mineral lineation. Large-scale shear zones were not observed in the area studied, but only small-scale high-angle shear zones (dextral or sinistral) occurring in single or conjugated sets bisected by the foliation. In both the Arco Verde tonalites and Guarantã monzogranite, the structural elements (foliation, lineation, syn-magmatic folds and shear-zones, conjugate shear-zones, tension gashes, boudinaged and folded veins) are in a spatial array consistent with a coaxial deformation. Finite deformation analysis points to a predominant flattening. All these data lead to the following conclusions:

1. The AVT and Guarantã monzogranite suffered a strong shortening under conditions ranging from high-T (near solidus and subsolidus ductile deformation; intense quartz and feldspar recrystallization) to low-T (low-grade brittle deformation; weakly recrystallized quartz, undulose extinction in feldspars).

2. The AVT and Guarantã monzogranite are not metamorphic rocks recrystallized under a prograde event, as previously suggested (e.g. Docegeo, 1988; Araújo et al., 1994), but syntectonic plutons. The Rio Maria granodiorites and Mata Surrão monzogranites, almost undeformed, postdate the deformation event.
3. Deformation recorded in the Arco Verde tonalites and Guarantã monzogranite corresponds to a flattening. Data suggest that the principal shortening axis is nearly horizontal and oriented N10–20°E (Fig. 8), whereas the extension direction is nearly horizontal and displays the same orientation as the foliation, where it can be determined.
4. The attitude of the foliation always steeply dipping towards the contacts, and evidence of an horizontal magmatic fabric locally preserved in the central part of the massif may suggest that the AVT unit is dome-shaped. This may be interpreted as the result of either diapiric ascent of magma, or of magma emplacement through fractures followed by ballooning (laccolithic plutons), interfering with the regional tectonic stress (e.g. Hutton, 1988; Clemens and Mawer, 1992; Pons et al., 1995; Petford, 1996).

5.2. Structure of the surrounding greenstone belts and the regional deformation

A comparison between the granitoids and related greenstones is essential for discussing the tectonic evolution of the Rio Maria terrain. Unfortunately, available data about greenstone belts remain scarce, and granite–greenstone contacts are mostly concealed (younger intrusives and discontinuous outcropping conditions).

In the Babaçu and Lagoa Seca greenstones (Fig. 1), Cordeiro and Saueressig (1980), Huhn (1991) report E–W trending structures consisting of a schistosity associated with asymetric folds with horizontal axes, and high-angle shear zones. Moreover, conjugated shear zones allow the orientation of the strain axes to be defined as follows: Z = N–S nearhorizontal, Y = vertical, X = E–W near-horizontal (Huhn, 1991), in close agreement with what is observed in the Arco Verde tonalites. In the Sapucaia greenstone belt, north of the Rio Maria terrain (Fig. 1), the schistosity is subvertical and displays the same orientation as the foliation of the surrounding Xingu 'gneisses'. The strain evolution is considered to have been controlled by a regional N–S shortening responsible for a dextral oblique reverse shearing (Oliveira et al., 1995). Structures of the Identidade greenstone belt (Fig. 1) were interpreted by Souza et al. (1988, 1996b) as a synform resulting from a dextral transpression, with shear zones related to a NS shortening direction. Souza et al. (1996b) further indicate that there is no unconformity between the structures of the greenstones and those of the granitoids.

Metamorphic phase assemblages in the greenstone belts do not allow the depth of emplacement of the Arco Verde tonalites to be estimated accurately (no Al–silicates). Nevertheless, Souza and Dall'Agnol (1994) report low-pressure greenschist-facies conditions in the Identidade greenstone belt, suggesting shallow emplacement conditions for the AVT.

In the greenstone belts, shear zones correspond dominantly to high-angle structures associated with overthrusting (Souza et al., 1988; Souza and Dall'Agnol, 1994), a pattern not observed in the Arco Verde tonalites. In these rocks, deformation corresponds dominantly to flattening with development of a strong foliation and vertical shear zones synchronous with magma emplacement, consolidation and cooling. The distinct structural patterns between greenstones and granitoids may simply express distinct rheological behaviours during a single tectonic event, or deviation of the foliation trajectories around rheological heterogeneities.

Available data converge to suggest that the structures of both the Andorinhas greenstones and the Arco Verde tonalites result from a same regional tectonic regime: (i) structures and style of deformation in the greenstones are conformable with those in the granitoids where it can be seen; and (ii) inferred strain axis orientations are similar in both the volcanosedimentary and plutonic units. This along with geochronological data suggest that the deposition and metamorphism of the volcano–sedimentary sequences (2979 ± 5,

2904 + 29/ − 22 Ma) along with the intrusion of the Arco Verde tonalites (2957) + 25/ − 21 Ma) and the Guarantã monzogranite (2.93 Ga) occurred in successive stages within a constant N–S transpressional regime.

5.3. Plutonism and Archaean tectonics

Two end-member tectonic structures and processes are reported for the growth and evolution of the Archaean crust (Choukroune et al., 1997; Collins et al., 1998).

1. Dome-and-basin structures related to buoyancy forces. These structures are considered to be due to partial convective overturn of the crust, reflecting the proximity of a plume within a craton submitted to weak boundary forces. There is no age zonality and granites form diapirs rimmed with greenstone belts. Typical examples are the Dharwar and east Pilbara cratons, and similar interpretations were also given for the Zimbabwe craton (e.g. Jelsma et al., 1993). For instance, in the Mount Edgar Batholith and adjacent Warrawoona Syncline (east Pilbara craton; Collins et al., 1998), the strain pattern across the granite-greenstone contact is characterized by a gradual change from an S-fabric (weak inclined flattening) to an intense L-fabric (in a radial array) towards the greenstone synclinal axis (strong vertical constrictional deformation). Closely similar structures are also reported in the Dharwar craton (with decollement horizons at the base of the greenstone belts interpreted in terms of progressive deformation), but a late intense transcurrent deformation ends the evolution of this area (Bouhallier et al., 1993; Choukroune et al., 1995; Chardon et al., 1998).
2. Fold-and-thrust structures related to regional-scale tangential tectonics. These structures reflect lateral accretion at the margins of a craton. There is a clear age zonality, and greenstone assemblages form slices resting tectonically on deeper crustal lithologies. This is, for instance, illustrated by the Superior Province in Canada (Choukroune et al., 1997), where structures encompasses a dominant nearly horizontal fabric, imbricated thick duplexes involving gneisses, granites, greenstones and sedimentary rocks (Pontiac subprovince; Camiré and Burg, 1993), and pervasive crustal-scale high temperature shearing and thrusting (Opatica Plutonic Belt; Sawyer and Benn, 1993). Late ubiquitous transcurrent shear zones are also observed.

The Rio Maria terrain presents some similarities with the east Pilbara craton and Superior Province: lithologies dominated by thick greenstone sequences and plutonic belts composed of TTG rocks, a large scale structure consisting of greenstone keels between gregarious batholiths, and a short time lag between greenstone eruption and granite emplacement and deformation. The large amounts of magma emplaced in a short time span in the Rio Maria area, along with dome-and-keel structures are consistent with intense reheating and thermal softening of the crust. However, the following two points have to be emphazised:

1. Although the overall geometry of the Rio Maria terrain consists of greenstone keels and synkinematic plutons, the structures are distinct from those reported in the east Pilbara and Dharwar cratons, and in the Superior Province as well. They consist mostly of subvertical. foliations, high-angle shear zones and subhorizontal stretching lineations with a constant direction, expressing an intense flattening in the granite domains and moderate transcurrent deformation in the greenstone belts. This suggests that, in the Rio Maria area, horizontal forces overcame gravitational instabilities, but that the crust was thermally softened allowing overall flattening rather than low-angle thrusting related to the convergence of rigid blocks.
2. Recycling of basement rocks in the genesis of Mount Edgar and Corunna Downs batholiths (east Pilbara. craton) appears clearly from field, geochronological and geochemical data, whereas the involvement of an older basement in the generation of the Rio Maria granitoids can only be suspected from zircon age data suggesting the presence of an older crust (3.0–3.2 Ga). The intrusive diatexites and high-

strain migmatites described in the Mount Edgar Batholith (suggesting that granitoids are still rooted in their rnigmatitic substrate) are lacking in the Rio Maria area where metamorphic recrystallizations are restricted to low-pressure greenschist-facies conditions (e.g. Souza and Dall'Agnol, 1994). This indicates that the Arco Verde tonalites and Guarantã monzogranite correspond to shallow level (unrooted?) plutons and that we have access to a crustal level higher than in east Pilbara. Further, although the overall geometry of the Rio Maria terrain is that of a dome-and-keel structure, this does not necessarily imply diapiric structures, because emplacement of magma along fractures with ballooning (giving raise to laccoliths) may also result in a strain pattern very similar to that produced by diapirism. In this respect, the Rio Maria area closely resembles the Chilimanzi granite suite in the Zimbabawe craton consisting of greenstone sequences intruded by upper crustal synkinematic plutons emplaced during a shortening event related to plate collision (e.g. Treloar and Blenkinsop, 1995).

In conclusion, the structural evolution of the Rio Maria terrain appears to represent an intermediate case between the east Pilbara craton dominated by diapiric movements, and the Superior Province characterized by thrust tectonics. The widespread transpressional deformation in the Rio Maria terrain suggests that strong external forces associated with plate convergence were operative between 2.96 and 2.90 Ga in the southeastern part of the Amazonian craton where intense horizontal shortening of a thermally softened crust shaped the granite–greenstone terrains.

Acknowledgements

Thanks to R. Dall'Agnol for logistic facilities and fruitful discussions during field work, and to M. Champenois for his assistance for finite strain analysis. Reviews by R. Caby and A Pimentel are gratefully acknowledged. We are indebted to P. Ledru for his detailed review and pertinent suggestions. This work benefited from financial support from the CNPq-Brazil (grant no. 202598/91-8 to F.A.), Centro de Geociências UFPA (Belém), CNRS (Missions Internationales), JE-249 (Université Henri Poincaré, Nancy) and CRPG-CNRS. This paper is CRPG contribution no. 1459.

References

Almeida, F.F.M., Hasui, Y., Brito Neves, B.B., Fuck, R., 1981. Brazilian structural provinces, an introduction. Earth Sci. Rev. 17, 1–29.

Althoff, F.J., Barbey, P., Boullier, A.M., Champenois, M., 1993. The Archaean evolution of a crustal segment over 100 Ma: the Amazonian craton. EUG VII, Strasbourg Terra Abstr. 5, 32.

Althoff, F.J., Barbey, P., Boullier, A.M., Dall'Agnol, R., 1994. Regime tectonico e composição dos granitóides arqueanos da região de Marajoara. IV Simp. Geol. Amazônia, Belém, pp. 291–294.

Althoff, F.J., Barbey, P., Dall'Agnol, R., Boullier, A.M., 1997. Metassedimentos arqueanos marcadores da evolução da crosta continental no cráton Amazônico. Congresso de Geoquímica dos Países de Língua Portuguesa, Braga, pp. 15–18.

Althoff, F.J., Barbey, P., Macambira, M., Scheller, T., Leterrier, J., Dall'Agnol, R., Lafon, J.-M., 1998. La croissance du craton sud-amazonien (région de Rio Maria, Brésil), Réunion Sci. Terre, Brest, Soc. Géol. Fr, Abstract, p. 62.

Araújo, O.J.B., Maia, R.G.N., 1991. Serra dos Carajás. Folha SB.22-Z-A. Texto explicativo. CPRM, Brasília, 150 pp.

Araújo, O.J.B., Maia, R.G.N., Jorge João, X.S., Costa, J.B.S., 1988. A megaestruturação arqueana da Folha Serra dos Carajás. Congresso Latino–Americano de Geologia, Belém 1, 324–337.

Araújo, O.J.B., Macambira, E.M.B., Vale, A.G., Oliveira, J.R., Silva Neto, C.S., Costa, E.J.S., Santos, A., Pena Filho, J.I.C., Neves, A.P., Jorge João, X.S., Costa, J.B.S., 1994. Primeira integração das investigações geológicas do programa grande Carajás na região SSE do estado do Parã. IV Simp. Geol. Amazônia, Belém, pp. 299–301.

Avelar, V.G., 1996. Geochronologia Pb-Pb, por evaporação em monocristal de zircão, do magmatismo da região de Tucumá, SE do Estado do Pará, Amazonia Oriental. Master thesis, Univ. Federal do Pará, Belém.

Barbosa, A.A., Lafon, J.-M., 1996. Geocronologia Pb–Pb e Rb–Sr de granitóides arqueanos da região de Redenção — sul do Pará. Rev. Brasil. Geoci. 26, 255–264.

Barker, F., 1979. Trondhjemite: definition, environment and hypotheses of origin. In: Barker, F. (Ed.), Trondhjemites, Dacites and Related Rocks, Develoments in Petrology, vol. 6. Elsevier, Amsterdam, pp. 1–12.

Barker, F., Arth, J.G., 1976. Generation of trondhjemitic-tonalitic liquids and Archaean bimodal trondhjemite-basalt suites. Geology 4, 596–600.

Barros, C.E.M., Dall'Agnol, R., Lafon, J.-M., Teixeira, N.P., Ribeiro, J.W., 1992. Geologia e geocronologia Rb–Sr do Gnaisse Estrêla, Curionópolis, PA. Boletim do Museu Paraense Emílio Goeldi. Ciências da Terra 4, 83–102.

Barros, C.E.M., Dall'Agnol, R., Barbey, P., Boullier, A.M., 1997. Geochemistry of the Estrela Granite Complex, Carajás region, Brazil: an example of an Archaean A-type granitoid. J. South Am. Earth Sci. 10, 321–330.

Beisiegel, V.R., Bernardelli, A.L., Drumond, N.F., Ruff, A.W., Tremaine, J.W., 1973. Geologia e recursos minerais da Serra dos Carajás. Rev. Brasil. Geosci. 3, 215–242.

Bouhallier, H., Choukroune, P., Ballèvre, M., 1993. Diapirism, bulk homogeneous shortening and transcurrent shearing in the Archaean Dharwar craton: the Holenarsipur area, souther India. Precambrian Res. 63, 43–58.

Camiré, G.E., Burg, J.P., 1993. Late Archaean thrusting in the northwestern Pontiac Subprovince, Canadian Shield. Precambrian Res. 61, 51–66.

Chardon, D., Choukroune, P., Jayananda, M., 1998. Sinking of the Dharwar basin (South India): implications for Archaean tectonics. Precambrian Res. 91, 15–39.

Choukroune, P., Bouhallier, H., Arndt, N.T., 1995. Soft lithosphere during periods of Archean crustal growth or crustal reworking. Geol. Soc. Spec. Publ. Lond. 95, 67–86.

Choukroune, P., Ludden, J.N., Chardon, D., Calvert, A.J., Bouhallier, H., 1997. Archaean crustal growth and tectonic processes: a comparison of the Superior Province, Canada and the Dharwar Craton, India. In: Burg, J.P., Ford, M. (Eds.), Orogeny Through Time, vol. 121. Geol. Soc. Spec. Publ, Londong, pp. 63–98.

Clemens, J.D., Mawer, C.K., 1992. Granitic magma transport by fracture propagation. Tectonophysics 204, 339–360.

Collins, W.J., Van Kranendonk, M.J., Teyssier, C., 1998. Partial convective overturn of Archaean crust in east Pilbara Craton, Western Australia: driving mechanisms and tectonic implications. J. Struct. Geol. 20, 1405–1424.

Condie, K.C., 1993. Chemical composition and evolution of the upper continental crust: contrasting results from surface samples and shales. Chem. Geol. 104, 1–37.

Cordeiro, A.A.C., Saueressig, R., 1980. Serra das Andorinhas: geologia e principais ocorrências de ouro, Congresso Brasileiro de Geologia, Camboriú (Abstr.), p. 344.

Costa, J.B.S., Araújo, O.J.B., Santos, A., Jorge João, X.S., Macambira, M.J.B., Lafon, J.M., 1995. A província mineral de Carajás: aspectos tectono-estruturais, estratigráficos e geocronológicos. IV Simp. Geol. Arnazônia, Belém, pp. 199–235.

Dall'Agnol, R., Lafon, J.-M., Macambira, M.J.B., 1994. Proterozoic anorogenic magmatism in the Central Amazonian Province, Amazonian Craton: geochronological, petrological and geochemical aspects. Mineral. Petrol. 50, 113–138.

Dias, G.S., Macambira, M.J.B., Dall'Agnol, R., Soares, A.D.V., Barros, C.E.M., 1996. Datação de zircões de sill de metagabro: comprovação da idade arqueana da Formação Aguas Claras, Carajás, Pará. IV Simp. Geol. Arnazônia, Belém, pp. 376–379.

Docegeo, 1988. Revisão litoestratigráfica da Província Mineral de Carajás. In: Província Mineral de Carajás: Litoestratigrafia e Principais Depósitos Minerais. Congr. Bras. Geol., Belém, Anexo, pp. 11–54.

Drummond, M.S., Defant, M.J., 1990. A model for trondhjemite-tonalite-dacite genesis and crustal growth via slab melting: Archaean to modem comparisons. J. Geophys. Res. 95, 21503–21525.

Duarte, K.D., Pereira, E.D., Dall'Agnol, R., Lafon, J.M., 1991. Geologia e geocronologia do Granito Mata Surrão — sudeste de Rio Maria (Pa). IV Simp. Geol. Arnazônia, Belém, p. 720.

Evensen, N.M., Hamilton, P.J., O'Nions, R.K., 1978. Rare-earth abundances in chondritic meteorites. Geochim. Cosmochim. Acta 42, 1199–1212.

Gibbs, A.K., Barron, C.N., 1983. The Guiana Shield reviewed. Episodes 2, 7–14.

Gibbs, A.K., Wirth, K.R., Hirata, W.K., Olzewski Jr, W.J., 1986. Age and composition of the Grão-Pará Group volcanics, Serra dos Carajás. Rev. Brasil. Geosci. 16, 201–211.

Huhn, S.R.B., 1991. Controle estrutural dos depósitos e ocorrências aurfferas no terreno granito greenstone da região de Rio Maria. III Symp. Geol. Arnazônia, Belém, pp. 211–219.

Huhn, S.R.B., Macambira, M.J.B., Dall'Agnol, R., 1999. Geologia e geochronologia Pb/Pb do granito alcalino Planalto, região da Serra do Rabo, Carajás, PA. VI Simp. Geol. Amazônia, Manaus, pp. 463–466.

Hutton, D.H.W., 1988. Granite emplacement mechanisms and tectonic controls; inferences from deformation studies. Trans. R. Soc. Edinburgh Earth Sci. 79, 615–631.

Jelsma, H.A., Van der Keek, P.A., Vinyu, M.L., 1993. Tectonic evolution of the Bindura–Shamva grenstone belt (Zimbabwe): progressive deformation around ballooning diapirs. J. Struct. Geol. 15, 163–176.

Johannes, W., Holtz, F., 1996. Petrogenesis and Experimental Petrology of Granitic Rocks. Springer Verlag, Berlin, 335 pp.

Johnston, A.D., Wyllie, P.J., 1988. Constraints on the origin of Archaean trondhjemites based on phase relationships of Nûk gneiss with H_2O at 15 kbar. Contrib. Mineral. Petrol. 100, 35–46.

Kisters, A.F.M., Anhaeusser, C.R., 1995. Emplacement features of Archaean TTG plutons along the southern margin of the Barberton greenstone belt, South Africa. Precambrian Res. 75, 1–15.

Lafon, J.-M., Rodrigues, E., Duarte, K.D., 1994. Le granite Mata Surrão: un magmatisme monzogranitique contemporain des associations tonalitiques-trondhjé-mitiques-granodioritiques archéennes de la région de Rio Maria (Amazonie orientale, Brésil). C. R. Acad. Sci. Paris 318, 643–649.

Lapique, F., Champenois, M., Cheilletz, A., 1988. Un analyseur vidéographique interactif: description et applications. Bull. Minéral. 111, 679–687.

Leake, B.E., Woolley, A.R., Birch, W.D., Gilbert, M.C., Grice, J.D., Hawthorne, F.C., Kato, A., Kisch, H.J., Krivovichev, V.G., Linthout, K., Laird, J., Mandarino, J., Mresch, W.V., Nickel, E.H., Rock, N.M.S., Schumacher, J.C., Smith, D.C., Stephenson, N.C.N., Ungaretti, L., Whittaker, E.J.W., Youzhi, G., 1997. Nomenclatures of amphiboles. Report of the Subcommittee on Amphiboles of the International Mineralogical Association Commission on New Minerals and Mineral Names. Eur. J. Mineral. 9, 623–651.

Lindenmayer, Z.G., Laux, J.H., Viero, A.C., 1995. O papel da alteração hidrotermal nas rochas da bacia de Carajás, Boletim do Museu Paraense Emílio Goeldi. Série Ciências da Terra 7, 125–145.

Macambira, M.J.B., Lafon, J.M., 1995. Geocronologia da província mineral de Carajás; síntese dos dados e novos desafios, Boletim do Museu Paraense Emílio Goeldi. Sèrie Ciências da Terra 7, 263–288.

Macambira, M.J.B., Lancelot, J., 1991. História arqueana da região de Rio Maria, SE do estado do Pará, registrada em zircões detríticos de greenstone belt e de cobertura plataformal. III Simp. Geol. Amazônia, Belém, pp. 59–69.

Macambira, M.J.B., Lancelot, J., 1992. Idade U–Pb em zircões de metavulcânica do greenstone do Supergrupo Andorinhas; delimitante da estratigrafia arqueana de Carajás, Estado do Pará. Congr. Bras. Geol., São Paulo 2, 188–189.

Macambira, M.J.B., Lancelot, J., 1996. Time constraints for the formation of the Archean Rio Maria Crust, Southeastern Amazonian Craton. Brazil. Int. Geol. Rev. 38, 1134–1142.

Macambira, M.J.B., Lafon, J.M., Barradas, J.A., 1991. Le granite de Xinguara, témoin d'un magmatisme monzogranitique dans l'archéen de l'Amazonie orientale, Brésil. C. R. Acad. Sci. Paris 313, 781–785.

Machado, N., Lindenmayer, Z., Krogh, T.E., Lindenmayer, D., 1991. U–Pb geochronology of Archean magmatism and basement reactivation in the Carajás area, Amazon shield, Brazil. Precambrian Res. 49, 329–354.

Magalhães, M.S., Figueiredo, M.A.M.B., Althoff, F.J., 1994. Comportamento magnético do tonalito Arco Verde e do granito Guarantã, Rio Maria, Pará: suscetibilidade magnática e minerais opacos. IV Simp. Geol. Amazônia, Belém, pp. 347–348.

Martin, H., 1987. Petrogenesis of Archaean trondhjemites, tonalites and granodiorites from Eastern Finland: major and trace element geochemistry. J. Petrol. 28, 921–953.

Martin, H., 1993. The mecanisms of petrogenesis of the Archaean continental crust-comparison with modem processes. Lithos 30, 373–388.

Martin, H., 1994. The Archean grey gneisses and the genesis of continental crust. In: Condie, K.C. (Ed.), Developments in Precambrian Geology, Archean Crustal Evolution, vol. 11. Elsevier, Amsterdam, pp. 205–259.

Medeiros, H., Gastal, M.C.P., Dall'Agnol R., Souza, Z.S., 1987. Geology of the Rio Maria area (Eastern Amazonian region — Brazil): an example of Archean granite–greesntone terrane intruded by anorogenic granites of Middle Proterozoic age. In: Precambrian evolution of the Amazonian region. Final Meeting of the Working Group, Carajás, IGCP Project 204, pp. 97–109.

Moser, D.E., 1994. The geology and structure of mid-crustal Wawa gneiss domain: a key to understanding tectonic variation with depth and time in the late Archean Abitibi-Wawa Orogen. Can. J. Earth Sci. 31, 1064–1080.

Mougeot, R., 1996. Etude de la limite Archéen-Protérozoique et des minéralisations Au $+/-$ U associées. Exemples de la région de Jacobina (Etat de Bahia, Brésil) et de Carajás (Etat de Para, Brésil). Unpublished thesis, University of Montpellier II, 301 p.

Nutman, A.P., Bennett, V.C., Friend, C.R.L., Norman, M.D., 1999. Meta-igneous (nongneissic) tonalites and quartz-diorites from an extensive ca. 3800 Ma terrain south of the Isua supracrustal belt, southern West Greenland: constraints on early crust formation. Contrib. Mineral Petrol 137, 364–388.

Oliveira, C.G., Santos, R.V., Leonardos, O.H., 1995. Geologia e ntineralizações aurfferas do greenstone belt Sapucaia sudeste do Pará. Boletim do Museu Paraense Emílio Goeldi 7, 61–91.

Panozzo, R.H., 1984. Two-dimensional strain from the orientation of lines in a plane. J. Struct. Geol. 6, 215–221.

Petford, N., 1996. Dykes or diapirs? Trans. R. Soc. Edinburgh Earth Sci. 87, 105–114.

Pimentel, M.M., Machado, N., 1994. Geocronologia U–Pb dos terrenos granito-greenstone de Rio Maria, Pará. Congresso Brasileiro de Geologia, Camborid, pp. 390–391.

Pons, J., Barbey, P., Dupuis, D., Léger, J.M., 1995. Mechanism of pluton emplacement and structural evolution of a 2.1 Ga juvenile continental crust: The Birimian of southwestern Niger. Precambrian Res. 70, 281–301.

Rapp, R.P., 1991. Origin of Archean granitoids and continental evolution. EOS 72, 225–229.

Rapp, R.P., Watson, E.B., 1995. Dehydration melting of metabasalt at 8–32 kbar: implications for continental growth and crust–mantle recycling. J. Petrol. 36, 891–931.

Rodrigues, E.S., Lafon, J.-M., Scheller, T., 1992. Geocronologia Pb–Pb da Província Mineral de Carajás: primeiros resultados. Congresso Brasileiro de Geologia, São Paulo 2, 183–184.

Sato, K., Tassinari, C.C.G., 1997. Principais eventos de acreção continental no Cráton Amazônico baseados ern idade-modelo Sm-Nd, calculada ern evoluções de estágio único e estdáio duplo. In: Costa, M.L., Angélica, R.S. (Eds.), Contribuições à Geologia da Amazônia. FINEP-SBG/NO, Belém, pp. 91–142.

Sawyer, E.W., Benn, K., 1993. Structure of the high-grade Opatica belt and adjacent lowgrade Abitibi subprovince and Archaean mountain front. J. Struct. Geol. 15, 1443–1458.

Silva, G.G., Lima, M.I.C., Andrade, A.R.F., Issler, R.S., Guimarães, G., 1974. Geologia. In: Folha SB 22 Araguaia e Parte da SC.22 Tocantins. Levantamento de Recursos Naturais, vol. 4. DNPM-Projeto Radam, Rio de Janeiro.

Souza, Z.S., Dall'Agnol, R., 1994. Metamorfismo de baixo grau no 'greenstone belt' de Identidade, região de Xinguara-Rio Maria, SE do Pará. IV Simp. Geol. Amazônia, Belém, pp. 387–390.

Souza, Z.S., Santos, A.B., Ledsham, E.J., Martins, L.P.B., Huhn, S.R.B., Costa, V.G., 1988. Feições geológicas e estruturais do 'greenstone belt' de Identidade, região de Xinguara-Rio Maria, sul do Pará. Congresso Brasileiro de Geologia, Belém 3, 1453–1467.

Souza, Z.S., Medeiros, H., Althoff, F.J., Dall'Agnol, R., 1990. Geologia do terreno "granitogreenstone" da região de Rio Maria, sudeste do Pará. Congresso Brasileiro de Geologia, Natal 6, 2913–2928.

Souza, S.R.B., Macambira, M.J.B., Scheller, T., 1996a. Novos dados geocronológicos para os granitos deformados do rio Itacaiúnas (Serra dos Carajás, PA); implicações estratigráficas. V Simp. Geol. Amazônia, Belém, pp. 380–382.

Souza, Z.S, Dall'Agnol, R., Althoff, F.J., Leite, A.A.S., Barros, C.E.M., 1996b. Carajás mineral province: geological, geochronological and tectonic contrasts on the Archean evolution of the Rio Maria granite–greenstone terrain and the Carajás block. Symposium Archaean terranes of the South American Platform, Brasilia, pp. 31–32.

Taylor S.R., McLennan, S.M., 1985. The Continental Crust: its Composition and Evolution. Blackwell, Oxford, 312 pp.

Teixeira, W., Tassinari, C.C.G., Cordani, U.G., Kawhasita, K., 1989. A review of the geochronology of the Amazonian Craton; tectonics implications. Precambrian Res. 42, 213–227.

Treloar, P.J., Blenkinsop, T.G., 1995. Archaean deformation patterns in Zimbabwe: true indicators of Tibetan-style crustal extusion or not? In: Cowards, P.P., Ries, A.C. (Eds.), Early Precambrian Processes, vol. 95. Geol. Soc. Spec. Publ, London, pp. 87–108.

Trendall, A.F., Basei, M.A.S., De Laeter, J.R., Nelson, D.R., 1998. SHRIMP zircon U–Pb constraints on the age of the Carajás formation, Grão Pará Group, Amazon craton. J. South Am. Earth Sci. 11, 265–277.

Vanderhaeghe, O., Ledru, P., Thiéblemont, D., Egal, E., Cocherie, A., Tegyey, M., Milési, J.P., 1998. Contrasting mechanism of crustal growth. Geodynamic evolution of the Paleoproterozoic granite–greenstone belts of French Guyana. Precambrian Res. 92, 165–193.